Indian Journal of Science and Technology, Vol 10(12), DOI: 10.17485/ijst/2017/v10i12/107464, March 2017
ISSN (Print) : 0974-6846
ISSN (Online) : 0974-5645

Effect of Rh Addition to Ni/MgO-Al_2O_3 Catalysts for Dry Reforming of Methane

Marco Antonio Ocsachoque*, Maria Silvia Leguizamon Aparicio and Maria Gloria Gonzalez

Departamento de Quimica. Facultad de Ciencias Exactas (UNLP), Centro de Investigacion y Desarrollo en Ciencias Aplicadas "Dr Jorge J. Ronco". (CONICET, CCT La Plata), 48 Nº 257 C.P. 1900, La Plata, Buenos Aires, Argentina;
ocmarco@quimica.unlp.edu.ar, marysylvhia@quimica.unlp.edu.ar, mgg@quimica.unlp.edu.ar

Abstract

Objective: This study has analyzed the performance of Ni and Ni-Rh catalysts based on MgO/g-Al_2O_3 in the process of dry reforming of methane (DRM). **Methods/Statistical Analysis:** The samples were prepared using the incipient wetness impregnation method and were characterized by N_2 adsorption, X-ray diffraction (XRD), temperature-programmed reduction (TPR), diffuse reflectance spectroscopy (DRS), surface acidity, X-ray photoelectron spectroscopy (XPS), thermal gravimetric analysis (TGA), and Raman spectroscopy. The catalysts were reduced with hydrogen and measured in the reaction of CH_4 with CO_2 at two CH_4/CO_2 ratios. **Findings:** The 0.5% Rh addition to Ni/MgO-g-Al_2O_3 improves the activity and the stability for this process. In the bimetallic catalysts, the reduction temperature of the active phase decreases due to the hydrogen spillover mechanism from the noble metal to the catalyst surface, which favors their catalytic activity. On the other hand, the interaction between Rh and the support would be the cause for the better performance of bimetallic catalysts. The Rh-Ni/MgO-g-Al_2O_3 catalyst is the most active, indicating that the impregnation order affects the catalytic behavior. **Improvements/Applications:** This study gives promising results for this type of catalyst, also showing the effect of the catalyst preparation on the activity and its relationship with deactivation by coke.

Keywords: Dry Reforming of Methane, Oxides, Rh-Ni Catalysts, Raman Spectroscopy and Scattering, Surface Properties

1. Introduction

Methane dry reforming is a very important reaction because it synthesizes gas with a H_2/CO ratio near the unit. This value is the adequate for the synthesis of valuable hydrocarbons for the industry. This process is very important from the environmental point of view, because both CH_4 and CO_2 are undesirable greenhouse gases that may be converted into products of industrial interest.

The catalysts most commonly used in this process are Ni catalysts due to their high availability and low cost, but they involve catalyst deactivation. It is known that carbon deposition and the sintering of metal particles on these catalysts have a noticeable negative effect on their catalytic behavior, which are the causes of catalyst deactivation. With respect to these problems, some papers[1-3] has indicated that the catalytic performance of Ni-based catalysts is improved by the addition of alkaline-earth or rare-earth metal oxides. Several authors have reported that the alkaline MgO support favors CO_2 absorption improving carbon resistance[4-6], it is known that the interaction of Ni^{+2} with the γ-Al_2O_3 affects catalyst reducibility and stability. This property of Ni catalysts is modified by the addition of small amounts of noble metal, in particular Rh or Pt[7,8]. Different authors[9-11] suggested that the performance of rhodium catalysts is mainly determined by accessible surface Rh atoms that catalyze methane decomposition followed by CO_2 reduction. On the other hand the addition of Rh favored the reducibity the NiMgO catalyst[12].

On these bases, this work analyzes the effects produced by the promotion of the Ni active phase by small Rh amounts, the modification of γ-Al_2O_3 with MgO, and the impregnation order of the active phase on the activ-

*Author for correspondence

ity, stability and carbon deposition during methane dry reforming.

2. Materials and Methods

2.1 Preparation of Catalysts

The modified support was synthesized by wetness impregnation of γ-Al_2O_3 (Rhône-Poulenc, Sg= 278 m^2g^{-1}, Vp= 0.340 cm^3g^{-1}) with a $Mg(NO_3)_2.6H_2O$ solution (3 wt% MgO), previous drying at 100°C, and calcination at 650°C for 1 h. A series of bimetallic catalysts with 0.5 wt% Rh and 5 wt% Ni was prepared by wetness impregnation of the modified support (MgO-γ-Al_2O_3) with aqueous solution of $Ni(NO_3)_2$ and $RhCl_3$. First, the MgO-γ-Al_2O_3 was impregnated with Rh and calcined at 650°C for 1 h. Then, the Ni solution was added and it was calcined at 650°C for 1 h. To compare the impregnation order of metals, another sample was prepared varying the addition order of metals; first, the MgO-γ-Al_2O_3 was impregnated with Ni and calcined at 650°C and then with Rh and calcined at 650°C, thus obtaining the respective series of catalysts: Ni-Rh/MgO-Al_2O_3 and Rh-Ni/MgO-Al_2O_3. Monometallic catalysts were synthesized with the same technique. The catalysts were named M/Mg (x)Al (M=Rh,Ni), where x indicates the Mg content (wt%). Before reaction, the catalysts were reduced with pure hydrogen at 650°C for 1h at a heating rate of 10°C/min.

2.2 Characterization of Catalysts

Samples were examined by N_2 adsorption, XRD, TPR, DRS, surface acidity, XPS, TGA, and Raman spectroscopy to analyze their properties and their effect on the catalytic activity, focusing on deactivation problems.

N_2 adsorption was carried out in ASAP 2020 Micromeritics equipment by nitrogen adsorption at -196°C. Previously, the samples were outgassed at 100°C for 12 h. The specific surface area was calculated using the BET method, and the pore volume was registered at P/P^o = 0.98.

The crystalline species were identified by XRD using Philips PW 1740 equipment, with CuKα radiation, operated at 40 kV and 20 mA. The range studied was 5°–70°, and the scan speed was 2°/min. Before characterization, the catalysts were reduced in hydrogen stream. The reducibility of samples was analyzed in TPR home- maid equipment with a TCD detector, using 100 mg of sample. In the experiments 10% H_2 in N_2 used was, and the heating rate was 10°C/min from 50°C to 900°C. DRS spectra were obtained in UV-VIS Varian Spectrophotometer, with a diffuse reflectance chamber with integrating sphere. The range studied was 200–800 nm using $BaSO_4$ as reference.

The acid properties of the samples were determinated by potentiometric titration with n-butylamine. A known amount of catalyst was suspended in acetonitrile with stirring. Subsequently, this suspension was titrated with a 0.025N n-butylamine solution in acetonitrile at a flow rate of 0.05 ml/min. The electrode potential variation was measured with a digital Instrumentalia pH-meter, using an Ag/AgCl electrode. XPS analyses were performed in multi-technique equipment (UniSpecs) with a dual X-ray source of Mg/Al and hemispherical analyzer PHOIBOS 150 in the fixed analyzer transmission (FAT) mode.

Samples were previously treated with a H_2/Ar mixture at 400°C for 10 min in the pretreatment chamber. These are the maximum temperature and time conditions permitted by the instrument. Spectra were obtained using an Mg anode operated at 200 W. The pressure during measurements was lower than $5x10^{-8}$ mbar. The binding energy of the C1s peak at 284.6eV was taken as reference.

Catalytic runs were conducted in a fixed-bed quartz reactor at 650°C and atmospheric pressure under chemical control conditions. The tubular reactor (Θ = 8 mm) was charged with 0.03 g of sample. The total gas flow was of 100 cm^3/min (CH_4:CO_2:He = 7:14:79). Catalytic stability tests were carried out for 20 h with a CH_4/CO_2 = 0.5 ratio at 650°C. Under these conditions the spontaneous carbon deposition is inhibited. Catalytic tests at the same conditions feeding the reactor with a total flow of 100 cm^3/min (CH_4:CO_2:He = 18:15:67) and CH_4/CO_2 ratio of 1.2 were performed to analyze carbon deposition.

Reactants were analyzed in Perkin-Elmer Sigma 1 gas chromatograph at 40°C through a column packed with Porapack Q, using a TCD and helium as carrier gas (20 cm^3/min). The mixture components, CO, H_2, CH_4, and CO_2, were separated under these conditions. The water contained in the stream was retained by a silica gel column.

The type and the percentage of carbon accumulated on the catalysts after 20 h on stream were determined by TGA and Raman spectroscopy. The thermogravimetric analysis was carried out in a Shimadzu TG 50 thermo balance under air stream at a heating rate of 20°C/min from room temperature to 900°C.

The Raman spectra were obtained with Via Renishaw spectrometer equipped with CCD detector and using an

excitation wavelength of 488.0 nm of an Ar^+ laser. The different spectroscopic parameters were determined after background subtraction by a curve fitting procedure with mixed Gaussian–Lorentzian functions using variable positions, FWHM, and intensities.

3. Results and Discussion

3.1. Textural Properties

Table 1 summarizes the S_{BET} and pore volume of the supports, fresh and used catalysts, to analyze the effect of promoter addition. The results show that MgO addition significantly decreases γ-Al_2O_3 surface area, which can be associated to the collapse of the MgO-γ-Al_2O_3 support during the precalcination at high temperature. However, after impregnation with MgO-Al_2O_3 and calcinations, only a slight decrease in the specific surface area of the materials was observed. Therefore, the textural parameters of fresh catalysts reduced at 650°C were defined by the MgO-Al_2O_3 modified support. On the other hand, the surface area and pore volume of used samples were lower than that of fresh catalysts.

Table 1. Morphological Properties of Catalysts

Materials	Sg(m^2/g)	Vp(cm^3/g)
γ- Al_2O_3	278	0.334
MgO(3)/γ-Al_2O_3	193	0.334
Ni(5)/γ-Al_2O_3 (fresh)	187	0.360
Ni(5)/Mg(3)-γ-Al_2O_3 (fresh)	179	0.320
Ni(5)/Mg(3)-γ-Al_2O_3 (used)	142	0.291
Ni(5)-Rh(0,5)/Mg(3)γ-Al_2O_3 (fresh)	179	0.323
Ni(5)-Rh(0,5)/Mg(3)-γ-Al_2O_3 (used)	157	0.304
Rh(0,5)-Ni(5)/Mg(3)-γ-Al_2O_3 (fresh)	178	0.318
Rh(0,5)-Ni(5)/Mg(3)-γ-Al_2O_3 (used)	152	0.306

3.2. X-Ray Diffraction

Figure 1 shows the XRD patterns of reduced catalysts and the modified support. The XRD analysis of the modified support calcined at 650°C revealed the presence of γ-Al_2O_3 (JCPDS 29-0063) and MgO (JCPDS 4-0829). In this sample, it is difficult to identify $MgAl_2O_4$ as a component of the modified support because peaks overlap each other. XRD profiles of all reduced catalysts showed characteristic peaks at 44.5° and 51.2° attributed to Ni° (JCPDS 4-0850). Characteristic Rh peaks were not observed in any of the catalysts probably due to the low metal content.

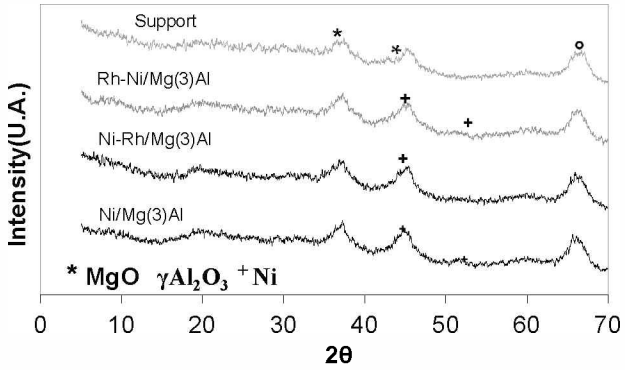

Figure 1. XRD patterns of Reduced Catalyst.

3.3. Temperature-Programmed Reduction

TPR experiments were performed to study the reducibility of the active phase in order to correlate the species present in these samples with the catalytic properties for the DRM reaction. Figure 2 depicts the TPR profiles obtained for the catalysts. The monometallic Ni/Mg(3)Al catalyst (Figure 2A) shows a reduction peak at 774°C, attributed to the reduction of NiO with an strong interaction with the support. This interaction could be produced by a solid solution between NiO and the surface support, forming a Ni aluminate. Additionally, two signals at low temperature were assigned to the reduction of NiO to Ni° and to the reduction of Ni interacting with the support. In the TPR profile of NiRh/Mg(3)Al sample (Figure 2B) two wide bands with Tmax at 500 and 750 °C were observed. These signals could be assigned to the reduction of NiO interacting with the alumina and to reduction of MgO-NiO solid solution, as in the case of the monometallic sample[13]. In addition, a defined peak was observed at 240°C, attributed to the reduction of Rh and Ni oxidized species.

The RhNi/Mg(3)Al catalyst, which was first impregnated with Ni (Figure 2C) presents a region containing two peaks of low intensity below 400°C and a large peak at 500°C with a wide shoulder at higher temperature. Signals at low temperature could be assigned to the reduction of metallic oxidized species.

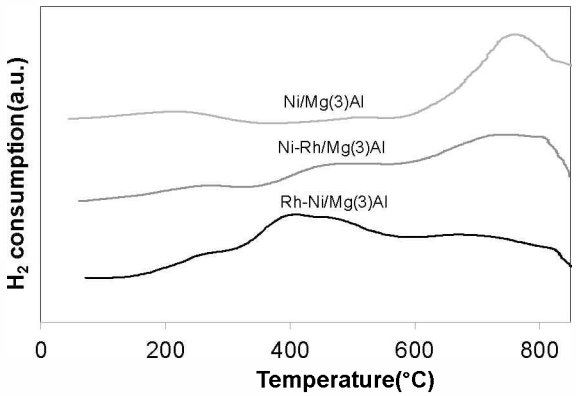

Figure 2. TPR Patterns of the Catalysts Calcined at 650°C.

In both bimetallic catalysts, the peak at 500°C shifts to lower temperature with respect to the monometallic sample. This decrease of the reduction temperature can be related to the presence of Rh, which promotes the reducibility of the catalyst by a hydrogen spillover mechanism from the noble metal to the bimetallic catalyst surface[13-15].

As the MgO content increases to 5 wt% (TPR not shown), both bimetallic catalysts show a stronger interaction between nickel oxide and the support. In the RhNi sample, a peak at 870°C and a shoulder at lower temperature are observed. The peak above 800°C is indicative of the strong metal-support interaction of NiO species with the support[16]. In the NiRh sample, a peak appears at around 750°C. The Ni reduction in either $MgAl_2O_4$ or $NiAl_2O_4$ spinel may occur at about 750°C[17,18]. It has been reported that the relatively stable form of $MgAl_2O_4$ prevents the formation of an inactive $NiAl_2O_4$ compound[17].

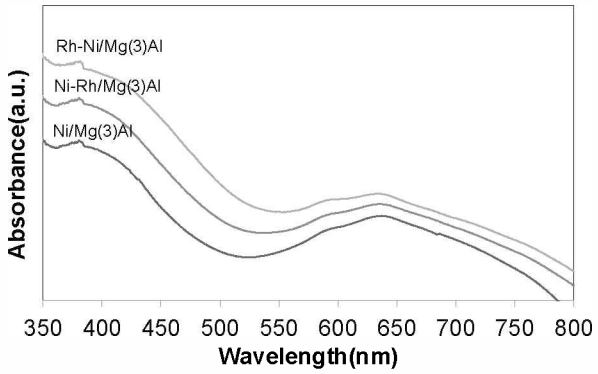

Figure 3. DRS Spectra of Unreduced Samples.

3.4. DRS Analysis

UV-Vis spectra of unreduced catalysts are shown in Figure 3. All samples show an absorption band at 380 nm, which can be attributed to d-d transitions of Ni(II) with octahedral symmetry in NiO. In addition, all samples present slight absorption bands between 590 and 640 nm, which can be attributed to transition d-d bands corresponding to Ni with octahedral symmetry in $NiAl_2O_4$. According to the results, it is possible to state that these samples are composed mainly of NiO and slightly of $NiAl_2O_4$. Probably, the presence of $MgAl_2O_4$ is responsible for the low $NiAl_2O_4$ concentration.

3.5. Surface Acidity

In order to estimate the acid properties of the catalysts, the potentiometric method with NBTA was used. In this titration, the initial electrode potential (E) indicates the strength of acid sites. In particular a sample with E < -100mV presents very weak sites.

The potentiometric titration curves in Figure 4 show the different acid-base properties of the catalysts studied. This figure also shows the effect of the impregnation order in bimetallic catalysts on the Lewis basicity of the samples under study. The Rh-Ni/MgAl catalyst presents the highest Lewis basicity if compared with the Ni/MgAl and Ni-Rh/MgAl samples. This property of the catalysts is of vital importance for their performance in the methane dry reforming process. Several authors have noted that carbon deposition can be attenuated by the basic strength of catalysts; therefore, the Rh-Ni/MgAl catalyst is expected to present the highest performance[19-21].

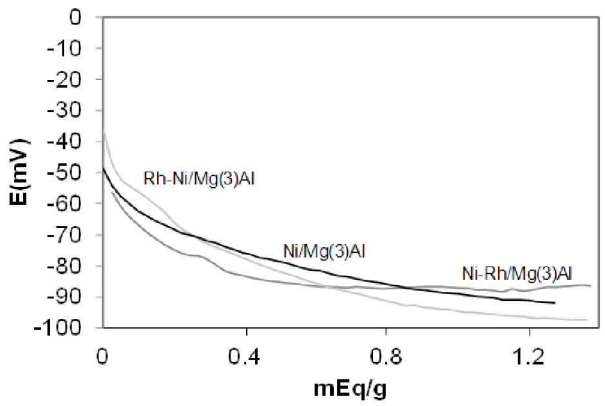

Figure 4. Potentiometric Titration Curves of Unreduced Samples.

3.6. XPS Analysis

In order to obtain information about the oxidation state of elements and surface composition, the catalysts were

analyzed by XPS. Samples were treated under H_2 flow at 650°C for 1 h and in the XPS equipment prechamber at 400°C; it is directly connected to the spectra acquisition chamber in order to avoid oxidation on the surface of metallic species during sample handling.

Figure 5 illustrates the spectra of the Ni 2p region for monometallic and bimetallic reduced catalysts. Two Ni species were detected for all samples; one at 852.2 eV related to Ni° and the other at 855.7 eV corresponding to Ni^{+2} [22,23], with a satellite signal at 861.9eV assigned to typical nickel species characteristic of $NiAl_2O_4$ spinel[24,25].

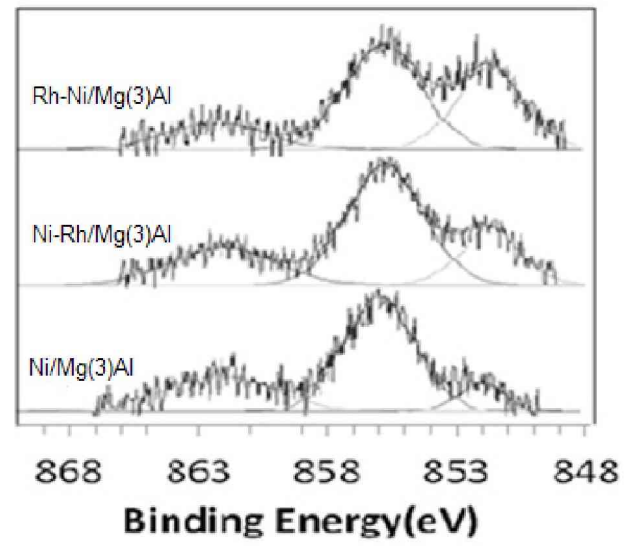

Figure 5. XPS Ni 2p Spectra of Reduced Catalyst.

These results would reveal that the surfaces of samples are not completely reduced after the reduction treatment. However, the Ni° fraction in the bimetallic catalysts is higher than in monometallic samples. This is in agreement with TPR, which indicates that Rh addition favors the reducibility of Ni oxide to Ni°. The deconvolution analysis of Ni 2p spectra shows that Ni^{+2} reducibility is increased by the addition of noble metal, from 22% for Ni to 37% and 70% for NiRh and RhNi, respectively.

In the Ni-Rh/MgAl catalyst, the spectra corresponding to the Rh 3d of bimetallic catalysts present two signals corresponding to Rh° $3d_{3/2}$ (306.1 eV) and Rh° $3d_{5/2}$ (311.4 eV)[24-26], and other peaks at 310.2 and 313.1 eV is corresponding to both oxidized Rh^{+n} species.

For the Rh-Ni/MgAl sample, two signals associated with Rh° (306.5 and 311.3 eV) were recorded, but no signals related to oxidize Rh were observed[27]. XPS analyses of RhNi/MgAl showed higher abundance of surface in Rh° species.

The surface atomic ratios of the different species are listed in Table 2. These results show that Rh addition increases Ni surface distribution.

Table 2. XPS Data of Mono- and Bi-Metallic Catalysts. Atomic Ratio.

Catalyst	(Ni/Mg+Al)	(Rh/Mg+Al)
Ni / Mg-Al	0.055	------
Ni-Rh/Mg-Al	0.063	0.00189
Rh-Ni/Mg-Al	0.065	0.00200

3.7. Catalytic Activity and Selectivity

In order to compare the reforming activity of different materials, experiments were carried out at 650°C with the same space velocity and feed composition. The catalytic properties of mono- and bi-metallic samples with Rh (0.5 wt%) and Ni (5 wt%) promoted with MgO(3 %wt) and calcined at 650°C were evaluated in the methane reforming with CO_2 at 650°C and CH_4/CO_2 = 0.5 molar ratio. Previously, the catalysts were treated under H_2 flow for 1 h at reaction temperature. The results of CH_4 conversion in the catalyst reaches a conversion constant are shown in Figure 6. By comparing monometallic and bimetallic catalysts, the results of reducibility suggest that the activity increases in bimetallic catalysts and can be related to the different reducibility of Ni due to the presence of Rh. In this sense, a synergistic phenomenon between Ni and Rh has been reported by others[12,26,28] and has been attributed to the promotion of Ni^{+2} reduction by hydrogen spillover from Rh.

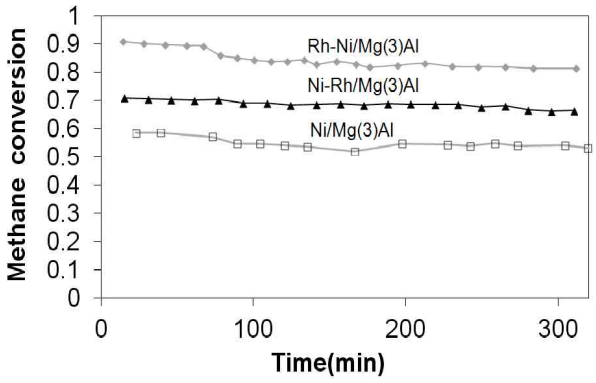

Figure 6. Methane Conversion at 650°C and CH_4/CO_2: 0.5 Ratio for Different Catalysts.

On the other hand, it is known that the reduction degree of the catalysts is an important factor affecting

their activity. In the case of RhNi/MgAl catalyst, the reduction degree probably increased, as confirmed by the lower reduction temperature and higher area of the TPR reduction peak. This fact could explain the high performance of this sample. For the case of NiRh/MgAl catalyst, the reduction temperature increased, therefore Ni^{+2} formation on $MgAl_2O_4$ spinel decreased the reducibility of Ni^{+2} to Ni^o, affecting the catalytic activity. Finally, the better behavior of the RhNi/MgAl catalyst with respect to the other samples is also associated with the greater content of active phase observed by XPS. Table 3 shows the selectivity to hydrogen expressed as the H_2/CO molar ratio. For all catalysts, this ratio was lower than one. So it is possible to infer that under these conditions the RWGS reaction ($CO_2 + H_2 \leftrightarrow CO + H_2O$) was favored, leading to higher CO production. In addition, when the metallic active phase is supported on a metal oxide with strong Lewis basicity, the catalyst ability of CO_2 increases, consequently the CO_2 can react with carbon to form CO, according to the reaction $CO_2 + C \leftrightarrow 2\ CO$. Both process produces to a lower H_2/CO molar ratio. The Ni/MgAl catalyst exhibited the lowest H_2/CO molar ratio, indicating the highest extension of both reactions.

Table 3. Selectivity to Hydrogen for the Catalysts at 650°C

Catalyst	H_2/CO molar ratio
Ni / Mg-Al	0.57
Ni-Rh/Mg-Al	0.61
Rh-Ni/Mg-Al	0.76

3.8. Catalytic Deactivation

At industrial level, it is desirable to operate with a CH_4/CO_2 ratio near the unit but, under this condition, carbon formation is thermodynamically favored. For this reason, the catalysts were tested at 650°C for 20 h using the CH_4/CO_2 = 1.2 ratio to analyze carbon deposition. Figure 7 shows methane conversion on the catalysts studied as a function of reaction time.

In bimetallic catalysts, catalytic tests showed a slight initial deactivation associated with carbon deposition. This behavior has been observed for RhNi/Al_2O_3 catalysts[29]. The Ni-MgAl catalyst also exhibited the same behavior. For this reason, the catalysts used were analyzed by TGO.

The amount of carbon accumulated on the used samples was measured by thermogravimetry in air stream at programmed temperature as is shown in Figure 8.

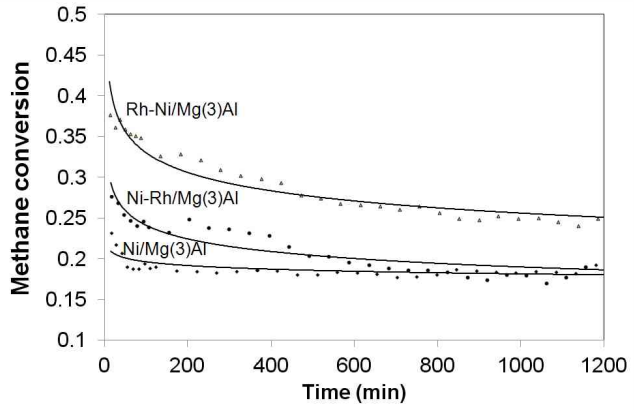

Figure 7. Methane Conversion at 650°C and CH_4/CO_2:1.2 Ratio.

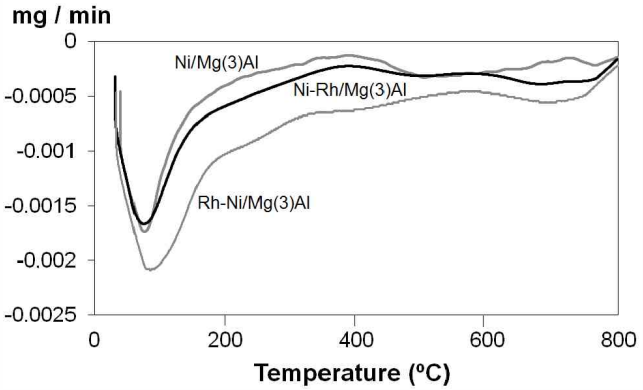

Figure 8. DTGA of Catalysts under Air Stream after 20 h Reaction.

The thermogravimetric diagrams show two types of carbonaceous species. Their oxidation temperature starts at 400°C, reaching maximums at around 510 and 700 °C. The signal at 510°C could be related to a surface carbon of whisker-filamentous type, and the signal at 700°C would correspond to a graphite type[30,31]. The former can be responsible for the mechanical destruction of the catalyst structure, while the latter blocks active centers resulting in catalyst deactivation. Both species can produce an irreversible deactivation. Some authors reported that carbons named C_β and C_γ are inactive species that show oxidation maximums at around 500 and 650 °C and are responsible for catalyst deactivation by carbon deposition[20,32]. The results obtained in terms of carbon content (Table 4) and in the determination of acid-base properties indicate that the Rh/Ni/MgAl catalyst is the one that presents the most basic strength and lowest carbon content. Several authors have reported that when the metal is supported on a metal oxide with strong Lewis basicity are observed changes in the carbon deposition. This behavior is due to increases in

the ability of catalysts to chemisorb CO_2 in the reforming of CH_4 with CO_2, and these species react with carbon to form CO, resulting in a lower amount of carbon.

Table 4. Carbon Deposition at 650°C

Catalyst	C_{dep}%(w/w)
Ni / Mg-Al	3.2
Ni-Rh/Mg-Al	4.3
Rh-Ni/Mg-Al	2.8

3.9. Raman Spectroscopy

In order to study carbon structures deposited on catalysts used in reaction, the Raman spectra of these samples were recorded.

The Raman spectra in Figure 9 of the catalysts have two main bands around 1346 cm^{-1} and 1520 cm^{-1}, associated with carbon. The band at 1520 cm^{-1} gives information about the electronic properties of filamentous carbon, indicating the presence of ordered carbon.

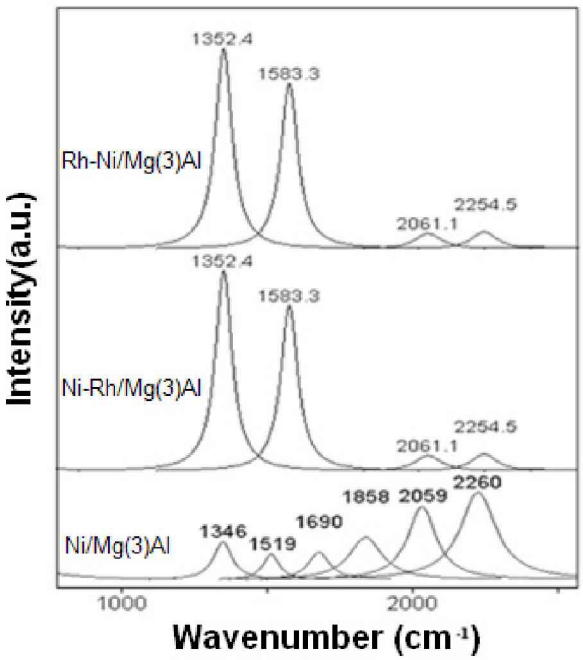

Figure 9. Deconvoluted Raman Spectra of Catalysts Extracted from the Reactor.

The band at 1346 cm^{-1} is associated with defective polycrystalline graphite and disordered structures and heteroatoms. Furthermore, the two bands observed between 2000 and 2300 cm^{-1} could be associated with structures presenting species of C≡C-type[33]. The Ni/MgAl catalyst has a band at 1620 cm^{-1}, associated with the organization degree of carbons. In addition, the absence of signals smaller than 300 cm^{-1} in the studied samples indicates the presence of multi-walled nanotubes (MWNT) as well as the appearance of a signal at around 1800 cm^{-1}, indicating the presence of single-wall nanotubes (SWNT).

4. Conclusions

The promotion of Ni/MgO-g-Al_2O_3 catalyst with Rh improves its activity and stability for the methane reforming with CO_2 after 20 h. The Rh-Ni/MgAl catalyst was the most active, indicating that the impregnation order affects the behavior of bimetallic catalysts. The results show that the surface distribution of metals (Ni and Rh) and metal reducibility would be determined by the impregnation order that influences the interaction between the active phase and the support. Thus, if the Rh is impregnated at the end, this interaction is weaker and consequently, the reducibility and the activity of the sample increase.

5. Acknowledgements

Authors thank CONICET, UNLP and ANPCyT for financing the purchase of the equipment "Multitecnica de superficies (PME 8–2003)" and for the economic help received to perform this work. Thanks are given to Eng. E. Soto and L. Osiglio for assistance in textural and superficial acidity measurements.

6. References

1. Takehira K, Shishido T, Wang P, Kosaka T, Takaki K. Autothermal reforming of CH4 over supported Ni catalysts prepared from Mg–Al hydrotalcite-like anionic clay. Journal of Catalysis. 2004 January; 221: 43–54. Crossref
2. Takanabe K, Nagaoka K, Nariai K, Aika K. Titania-supported cobalt and nickel bimetallic catalysts for carbon dioxide reforming of methane. Journal of Catalysis. 2005 June; 232: 268–75. Crossref
3. Koo KY, Roh HS, Seo YT, Seo DJ, Yoon WL, Park SB. A highly effective and stable nano-sized Ni/MgO–Al2O3 catalyst for gas to liquids (GTL) process. International Journal of Hydrogen Energy. 2008 April; 33: 2036–43. Crossref
4. Moon HD, Lim TH, Lee HI. Chemical poisoning of Ni/MgO catalyst by alkali carbonate vapor in the steam reforming reaction of DIR-MCFC. Bulletin of the Korean Chemical Society. 1999 October; 20: 1413–17.

5. Moon HD, Kim JH, Ha HY, Lim TH, Hong SA, Lee HI. Chemical poisoning of the Ni/MgO catalyst by alkali carbonate in a DIR-MCFC. Journal of the Korean Industrial Engineering Chemistry. 1999 October; 10: 754–60.
6. Zhu X, Huo PP, Zhang YP, Liu CJ. Characterization of Argon Glow Discharge Plasma Reduced Pt/Al2O3 Catalyst. Industrial and Engineering Chemistry Research. 2006 November; 45: 8604–09. Crossref
7. Li D, Nishida K, Zhan Y, Shishido T, Oumi Y, Sano T. Superior catalytic behavior of trace Pt-doped Ni/Mg(Al)O in methane reforming under daily start-up and shut-down operation. Applied Catalysis A: General. 2008 November; 350: 225–36. Crossref
8. Nakagawa K, Ikenaga N, Teng Y, Kobyashi T, Susuki T. Partial oxidation of methane to synthesis gas over iridium–nickel bimetallic catalysts. Applied Catalysis A: General. 1999 April; 180: 183–93. Crossref
9. Bitter JH, Seshan K, Lercher JA. Mono and Bifunctional Pathways of CO2/CH4 Reforming over Pt and Rh Based Catalysts. Journal of Catalysis.1998 May; 176: 93–101. Crossref
10. Aupretre F, Descorme C, Duprez D, Casanave D, Uzio D. Ethanol steam reforming over MgxNi1−xAl2O3 spinel oxide-supported Rh catalysts. Journal of Catalysis. 2005 July; 233: 464–77. Crossref
11. Ocsachoque MA, Pompeo F, González MG. Rh–Ni/CeO2–Al2O3 catalysts for methane dry reforming. Catalysis Today. 2011 August; 172: 226–31. Crossref
12. Chen Y-G, Tomishige K, Yokoyama K, Fujimoto K. Promoting effect of Pt, Pd and Rh noble metals to the Ni0.03Mg0.97O solid solution catalysts for the reforming of CH4 with CO2. Applied Catalysis A: General. 1997 December; 165: 335–47. Crossref
13. Rezaei M, Meshkani F, Biabani AB, Nematollahi B, Ranjbar A, Hadian N, Mosayebi Z. Autothermal reforming of methane over Ni catalysts supported on nanocrystalline MgO with high surface area and plated-like shape. International Journal of Hydrogen Energy. 2011 September; 36: 11712–17. Crossref
14. Juan-Juan J, Román-Martínez MC, Illán-Gómez MJ. Effect of potassium content in the activity of K-promoted Ni/Al2O3 catalysts for the dry reforming of methane. Applied Catalysis A: General. 2006 February; 301: 9–15. Crossref
15. Pena JA, Herguido J, Guimon C, Monzón A, Santamarina J. Hydrogenation of Acetylene over Ni/NiAl2O4Catalyst: Characterization. Coking and Reaction Studies. Journal of Catalysis. 1996 April; 159: 313–22. Crossref
16. Parmaliana A, Arena F, Frusteri F, Giordano N. Temperature-programmed reduction study of NiO–MgO interactions in magnesia-supported Ni catalysts and NiO–MgO physical mixture. Journal of the Chemical Society Faraday Transactions. 1990 January; 86: 2663–69. Crossref
17. Koo KY, Roh HS, Seo YT, Seo DJ, Yoon WL, Park SB. Coke study on MgO-promoted Ni/Al2O3 catalyst in combined H2O and CO2 reforming of methane for gas to liquid (GTL) process. Applied Catalysis A: General. 2008 June; 340: 183–90. Crossref
18. De Souza HSA, Da Silva AN, Castro AJR, Campos A, Filho JM, Oliveira AC. Mesoporous catalysts for dry reforming of methane: Correlation between structure and deactivation behaviour of Ni-containing catalysts. International Journal of Hydrogen Energy. 2012 September; 37: 12281–91. Crossref
19. Zhang ZL, Verykios XE. Carbon dioxide reforming of methane to synthesis gas over supported Ni catalysts. Catalysis Today. 1994 December; 21: 589–95. Crossref
20. Hourichi T, Sakuma K, Fukui T, Kubo Y, Osaki T, Mori T. Suppression of carbon deposition in the CO2-reforming of CH4 by adding basic metal oxides to a Ni/Al2O3 catalyst. Applied Catalysis A: General. 1996 September; 144: 111–20. Crossref
21. Kim GJ, Cho D, Kim K, Kim J. The reaction of CO2 with CH4 to synthesize H2 and CO over nickel-loaded Y-zeolites. Catalysis Letters. 1994 March; 28: 41–52. Crossref
22. Pino L, Vita A, Cipiti F, Lagana M, Recupero V. Hydrogen production by methane tri-reforming process over Ni–ceria catalysts: Effect of La-doping. Applied Catalysis B: Environmental. 2011 April; 104: 64–73. Crossref
23. Xu L, Song H, Chou L. Carbon dioxide reforming of methane over ordered mesoporous NiO–MgO–Al2O3 composite oxides. Applied Catalysis B: Environmental. 2011 October; 108–109: 177–90. Crossref
24. Suarez S, Yates M, Petre AL, Martin JA, Avila P, Blanco J. Development of a new Rh/TiO2–sepiolite monolithic catalyst for N2O decomposition. Applied Catalysis B: Environmental. 2006 May; 64: 302–11. Crossref
25. Ojeda M, Lopez Granados M, Rojas S, Terreros PF, Garcia-Garcia FJ, Fierro JLG. Manganese-promoted Rh/Al2O3 for C2-oxygenates synthesis from syngas: Effect of manganese loading. Applied Catalysis A: General. 2004 April; 261: 47–55. Crossref
26. Dohmae K, Nonaka T, Seno Y. Local structure change of Rh on alumina after treatments in high-temperature oxidizing and reducing environments. Surface and Interface Analysis. 2005 January; 37: 115–19. Crossref
27. Li H, Li HX, Dai WL, Wang WJ, Fang ZG. XPS studies on surface electronic characteristics of Ni–B and Ni–P amorphous alloy and its correlation to their catalytic properties. Applied Surface Science. 1999 November; 152: 25–34. Crossref
28. Larichev YV, Netskina OV, Komova OV, Simagina VI. Comparative XPS study of Rh/Al2O3 and Rh/TiO2 as catalysts for NaBH4 hydrolysis. International Journal of Hydrogen Energy. 2010 July; 35: 6501–07. Crossref

29. Lucredio AF, Assaf JM, Assaf EM. Methane conversion reactions on Ni catalysts promoted with Rh: Influence of support. Applied Catalysis A: General. 2011 June; 400: 156–65. Crossref
30. Ocsachoque M, Quincoces C, González MG. Effect of Rh addition on activity and stability over NI/γ-AL2O3 catalysts during methane reforming with CO2. Studies in Surface Science and Catalysis. 2007 May; 167: 397–402. Crossref
31. Pompeo F, Nichio NN, González MG, Montes M. Characterization of Ni/SiO2 and Ni/Li-SiO2 catalysts for methane dry reforming. Catalysis Today. 2005 October; 107: 856–62. Crossref
32. Hou ZY, Yokota O, Tanaka T, Yashima T. Investigation of CH4 Reforming with CO2 on Mesoporous Al2O3-Supported Ni Catalyst. Catalysis Letters. 2003 July; 89: 121–27. Crossref
33. Li S, Ji G, Huang Z, Zhang F, Du Y. Synthesis of chaoite-like macrotubes at low temperature and ambient pressure. Carbon. 2007 December; 45: 2946–50 Crossref